A proteomic approach links decreased pyruvate kinase M2 expression to oxaliplatin resistance in patients with colorectal cancer and in human cell lines

Eva Martinez-Balibrea,[1,3] Carmen Plasencia,[3] Alba Ginés,[1] Anna Martinez-Cardús,[1] Eva Musulén,[2] Rodrigo Aguilera,[3] José Luis Manzano,[1] Nouri Neamati,[3] and Albert Abad[1]

[1]Medical Oncology Service, Hospital Universitari Germans Trias i Pujol, Institut Catala Oncologia and [2]Department of Pathology, Hospital Universitari Germans Trias i Pujol, Badalona, Barcelona, Spain; and [3]Department of Pharmacology and Pharmaceutical Sciences, School of Pharmacy, University of Southern California, Los Angeles, California

Abstract

We aimed to gain further understanding of the molecular mechanisms involved in oxaliplatin resistance in colorectal cancer by using a proteomic approach. A 5-fold oxaliplatin-resistant cell line, HTOXAR3, was compared with its parental cell line, HT29, using two-dimensional PAGE. Mass spectrometry, Western blot, and real-time quantitative PCR confirmed the down-regulation of pyruvate kinase M2 (PK-M2) in HTOXAR3 cells. In a panel of eight colorectal cancer cell lines, we found a negative correlation between oxaliplatin resistance and PK-M2 mRNA levels (Spearman $r = -0.846$, $P = 0.008$). Oxaliplatin exposure in both HT29 and HTOXAR3 led to PK-M2 mRNA up-regulation. PK-M2 mRNA levels were measured by real-time quantitative PCR in 41 tumors treated with oxaliplatin/5-fluorouracil. Tumors with the lowest PK-M2 levels attained the lowest response rates (20% versus 64.5%, $P = 0.026$). High PK-M2 levels were associated with high p53 levels ($P = 0.032$). In conclusion, the data provided clearly link PK-M2 expression and oxaliplatin resistance mechanisms and further implicate PK-M2 as a predictive marker of response in patients with oxaliplatin-treated colorectal cancer. [Mol Cancer Ther 2009;8(4): 771–8]

Received 9/15/08; revised 12/18/08; accepted 1/26/09.

The costs of publication of this article were defrayed in part by the payment of page charges. This article must therefore be hereby marked *advertisement* in accordance with 18 U.S.C. Section 1734 solely to indicate this fact.

Note: Current address for C. Plasencia: Applied Research using Omic Sciences, S.L. (A05-B05), Parc Científic de Barcelona, Edifici Satèl·lit; Baldiri Reixac 15-21, 08028 Barcelona, Spain.

Current address for R. Aguilera: Applied Biosystems, 25 avenue de la Baltique, 91943 Courtaboeuf, France.

Requests for reprints: Albert Abad, Medical Oncology Service, Hospital Universitari Germans Trias i Pujol, Institut Catala Oncologia, Badalona 08916, Barcelona, Spain. Phone: 34-497-8925; Fax: 34-497-8950. E-mail: aabade@seom.org and Nouri Neamati, Department of Pharmaceutical Sciences, School of Pharmacy, University of Southern California, Los Angeles, CA 90033. E-mail: neamati@usc.edu

doi:10.1158/1535-7163.MCT-08-0882

Introduction

Colorectal carcinoma remains the second most common cause of cancer death in developed countries. Oxaliplatin, a diaminecyclohexane platinum, has shown activity against colorectal cancer in both chemotherapy-naïve patients and patients whose disease has progressed on 5-fluorouracil (5FU)–based therapy. In fact, the addition of oxaliplatin to 5FU/folinic acid regimens has increased objective response rates to >40% in patients with colorectal cancer. Still, major obstacles in the therapeutic use of platinum analogues are intrinsic or acquired resistance (1). Recently, there has been an increase in the understanding of the factors involved in these phenomena. Resistance is a multifactoral process that may include alteration in transport (uptake and efflux), drug detoxification, DNA repair, tolerance to DNA damage, and apoptosis (2–4). In addition, there are still major gaps in our understanding of the relationships among factors contributing to platinum resistance and their application in the clinic.

Proteomics studies allow the characterization and identification of potentially all the proteins in a cell as well as protein isoforms, modifications, and interactions (5). This approach may provide a better understanding of the molecular mechanisms involved in platinum resistance. This understanding is of paramount importance in devising future strategies to circumvent oxaliplatin resistance with the aim of increasing response rate and decreasing severe toxicities. In the present study, we sought to gain further insight into the mechanisms underlying oxaliplatin resistance. We established an oxaliplatin-resistant human colon cancer cell line and used both parental and resistant cells in comparative proteomics studies. Among the different proteins identified, we focused our attention on the down-regulation of pyruvate kinase isoform M2 (PK-M2) in resistant cells because it has recently been associated with the activation of apoptotic processes after cellular stress induction (6). We evaluated the potential role of PK-M2, not only related to the emergence of the oxaliplatin-resistant phenotype in HT29 cells, but also with its involvement in the clinical response of patients with colorectal cancer to 5FU plus oxaliplatin as first-line chemotherapy.

Materials and Methods

Cell Lines

Human colorectal carcinoma cell lines LS411N, LS513, and SW48 were obtained from American Type Culture

Collection. SW480, HCT116, LS174T, SW1417, and SW1116 cell lines were kindly provided by Dr. Francesc X. Real. Human tumor–derived colorectal cancer HT29 cells (American Type Culture Collection) were used as the parental cells to obtain the oxaliplatin-resistant subline HTOXAR3. HTOXAR3 was established as a result of continuous exposure to increasing concentrations of oxaliplatin as described previously (7). Cell lines were grown as monolayers in DMEM (HT29 and HTOXAR3; Invitrogen) or RPMI (Invitrogen) supplemented with 10% heat-inactivated FCS (Invitrogen), 400 units/mL of penicillin, 40 μg/mL of gentamicin, and 2 mmol/L of L-glutamine (Sigma) and cultured at 37°C in a humidified atmosphere of 5% CO_2. Cells were routinely checked for *Mycoplasma* contamination using a PCR-based assay (Stratagene). Resistant cells were stably resistant and maintained in oxaliplatin-free medium over a month previous to all experiments.

Drugs

Oxaliplatin, cisplatin, and SN-38 were prepared in water (10 mmol/L), physiologic serum (3 mg/mL), or DMSO (10 mmol/L), respectively, as stock solutions, and stored at −20°C. Further dilutions of each drug were made in culture medium to final concentrations before use.

Cell Viability Assay

The cytotoxicity of all drugs was assessed by the 3-(4,5-dimethylthiazol-2-yl)-2,5-diphenyltetrazolium bromide (MTT) assay (8). Cancer cells were seeded at a density of 2,000 cells per well in 96-well microtiter plates and allowed to attach. Cells were treated with continuous exposure to a corresponding drug for 24 h. Subsequently, the drug was removed and fresh medium was added to each well. Cells were allowed to grow for 72 h. MTT (Roche Diagnostics) was then added and doses for each fraction of survival (ranging from 10% to 90% of cell viability) were determined in each cell line by the median-effect line method. The data reported represent the mean ± SD of a minimum of three independent experiments done with eight wells at each drug concentration tested.

Patient Samples

Eligible patients were older than 18 years with histologically confirmed metastatic colorectal adenocarcinoma; performance status ≥2; and adequate bone marrow, renal, and hepatic functions. Previous cytotoxic chemotherapy was not permitted except for adjuvant treatment completed 12 mo before study enrollment. Response assessments were obtained according to Response Evaluation Criteria in Solid Tumors standards. Patients received oxaliplatin biweekly at 85 mg/m^2, i.v., 2 h, plus 48 h weekly continuous infusion of 5FU at 2,250 mg/m^2 (TTD schedule) with a maximum of 12 cycles. Treatment was continued until progressive disease, unacceptable toxicity, or consent withdrawal. The study protocol was approved by the local ethics committee and all subjects gave informed consent before inclusion in the study.

Two-Dimensional Gel Electrophoresis Analysis

Cells were harvested and allowed to reach ~60% confluence in culture flasks. They were then collected, washed in PBS, and pelleted. Proteins were extracted using ReadyPrep Sequential extraction kit (Bio-Rad) according to the instructions of the manufacturer. Two fractions of different solubilities were obtained. The protein content of each fraction was determined using the Bradford method. Protein samples were stored at −80°C until used. A total of 150 μg of proteins from each fraction were suspended in 0.3 mL of rehydration buffer [8 mol/L urea, 2% (w/v) CHAPS, 50 mmol/L DTT, 0.2% (w/v) Bio-Lyte 3/10 ampholyte, and traces of bromophenol blue] and loaded over dry IPG strips (17 cm, pH 3–10; Bio-Rad). The rehydration was done at 50 V, 20°C, for 12 to 16 h in a focusing tray (Bio-Rad). The focusing conditions were as follows: 10,000 V end voltage, 40,000 to 60,000 V/h (rapid ramp), 20°C. The focused strips were equilibrated as follows: 10 min in equilibration buffer I [6 mol/L urea, 2% SDS, 0.375 mol/L Tris-HCl (pH 8.8), 2% (w/v) DTT, and 20% glycerol] followed by a 10-min incubation in equilibration buffer II [6 mol/L urea, 2% SDS, 0.375 mol/L Tris-HCl (pH 8.8), 2.5% (w/v) iodoacetamide, and 20% glycerol]. For the second-dimension gel electrophoresis, the equilibrated strips were aligned on the top of a 12% polyacrylamide gel and sealed with 0.5% low-melting agarose. Protein separation was done at 16 mA/gel for 1 h followed by 24 mA/gel for 5 to 6 h. At the end of the run, gels were removed, washed in distilled water, and stained either with the SYPRO-Ruby Protein Gel Stain (Bio-Rad) or with silver stain (Bio-Rad) according to the protocols provided by the manufacturer. The gels were scanned using Typhoon 8610 (GE Healthcare) and the resulting images were processed using PDQuest 7.0 (Bio-Rad) to identify protein alterations in resistant/parental cell pairs. At least three independent experiments were done.

Protein Identification by Liquid Chromatography Tandem Mass Spectrometry

Protein spots from SDS-PAGE were excised using biopsy punches (Acuderm). Silver-stained bands were destained prior to an in-gel tryptic digest that was carried out using trypsin, which has been reductively methylated to reduce

Table 1 Antibodies, suppliers, dilutions, and techniques used for immunohistochemistry and variables evaluated

Antibody	Source	Dilution	Technique	Variables evaluated
Anti-human p53 protein (clone DO7), mouse monoclonal antibody	Novocastra	1:500	Dako Autostainer	Percentage
Anti-human bcl-2 oncoprotein, mouse monoclonal antibody	Dako	1:350	Ventana, Nexes	Immunoreactivity vs negative
Anti-human ki-67 (clone MIB-1), mouse monoclonal antibody	Dako	1:600	Dako Autostainer	Percentage

Table 2 Cytotoxicity of oxaliplatin, cisplatin, and SN-38 in HT29 and HTOXAR3

Cell line	OXA (μmol/L)		CDDP (μmol/L)		SN-38 (nmol/L)		5FU (μmol/L)	
	IC_{50} ± SD	RI	IC_{50} ± SD	RI	IC_{50} ± SD	RI	IC_{50} ± SD	RI
HT29	6.96 ± 0.85	4.71	4.70 ± 0.6	0.6	9.68 ± 0.07	1.07	13.02 ± 0.4	0.87
HTOXAR3	32.78 ± 5.32		2.70 ± 0.23		10.31 ± 0.52		12.59 ± 2.09	

Abbreviations: OXA, oxaliplatin; CDDP, cisplatin; RI, resistance index (IC_{50} resistant cells/IC_{50} sensitive cells).

autolysis (Promega). Prior to digestion, samples were reduced with DTT and alkylated with iodoacetamide. The digestion reaction was carried out overnight at 37°C. Chromatographic separation of the tryptic peptides was achieved using a ThermoFinnigan Surveyor MS-Pump in conjunction with a BioBasic-18 100 mm × 0.18 mm reverse phase capillary column (ThermoFinnigan). Mass analysis was done using a ThermoFinnigan LCQ Deca XP Plus ion trap mass spectrometer equipped with a nanospray ion source (ThermoFinnigan). The columns were equilibrated for 5 min at 1.5 μL/min with 95% solution A (0.1% acetic acid in water) and 5% solution B (0.1% formic acid in acetonitrile) prior to sample injection. Mass spectra were acquired in the m/z 400 to 1,800 range. Protein identification was done using the tandem mass spectrometry search software Mascot (Matrix Science) with confirmatory or complementary analyses using TurboSequest (Bioworks Browser v. 3.2). The National Center for Biotechnology Information human genome database server complemented with the National Center for Biotechnology Information nonredundant protein database were used for searching.

Western Blotting

Cells were homogenized in NP40 buffer [20 mmol/L Tris-HCl (pH 8), 137 mmol/L NaCl, 10% glycerol, 1% NP40, and 2 mmol/L EDTA] containing protease inhibitors (1 μg/μL phenylmethylsulfonyl fluoride, leupeptin, and pepstatin as well as 0.1 μg/μL aprotinin). Protein concentration homogenates were estimated by using the BCA kit (Pierce) with bovine serum albumin as standard. Ten micrograms of protein were loaded and subjected to SDS-PAGE. After electrophoresis, proteins were transferred to polyvinylidene difluoride membranes (Millipore), which were then blocked by incubating for 2 h at room temperature in 0.1% Tween 20-TBS containing 10% nonfat dry milk. Membranes were then incubated for 1 h at room temperature in continuous agitation with diluted primary antibodies against either PK-M2 (Abcam) or actin (Sigma). After washing in Tween 20-TBS, membranes were incubated with diluted horseradish peroxidase–containing secondary antibodies (Cell Signaling) for 1 h at room temperature. Membranes were washed and incubated with Immobilon Western chemiluminescence reagent (Millipore) for the appropriate times and exposed to film (Fujifilm, Super RX). Protein band densities were calculated by using ImageJ software v1.37 (NIH).[4]

[4] http://rsb.info.nih.gov/ij/

Quantitative Real-time PCR

We examined *PKM2* gene expression in formalin-fixed, paraffin-embedded tissue from 41 primary colorectal adenocarcinomas following a method, optimized for mRNA quantification in these kinds of samples, that has previously been described (9). The primer and probe sets for actin were designed using Primer Express 2.0 Software (Applied Biosystems) and were as follows: forward 5′-TGAGCGCGGCTACAGCTT-3′, reverse 5′-TCCTTAATGTCACGCACGATTT-3′, probe 5′-ACCACCACGGCCGAGCGG-3′. Quantification of gene expression was done using the ABI Prism 7900HT Sequence Detection System (Applied Biosystems). Primers and probes for PK-M2 mRNA expression analysis were purchased predesigned from Applied Biosystems (assay no. Hs00762869_s1). The PCR product size generated with these primers was 62 bp. Relative gene expression quantification was calculated according to the comparative Ct method as described elsewhere and using β-actin as an endogenous control and commercial RNA controls (Stratagene) as calibrators. In all experiments, only triplicates with a Ct value of 0.20 SD were accepted. In addition, for each sample analyzed, a retrotranscriptase minus control was run in the same plate to assure the absence of genomic DNA contamination. Gene expression analysis was also done on RNA from cells. Total RNA was obtained by using the RNeasy Mini Kit (Qiagen) and retrotranscribed as described above.

Tissue Microarray

The H&E-stained slides of all tumors were reviewed to identify the most well-preserved areas. Tissues corresponding to these areas were randomly sampled from paraffin blocks, with no special preference for the different parts of the tumor (e.g., superficial zone versus infiltrating border). Three cylindrical cores, each measuring 0.6 mm in diameter, were obtained from every donor block using a tissue microarray workstation MTA-1 (Beecher Instruments).

Antibodies and Immunohistochemical Studies

Five-micrometer-thick sections were deparaffinized, hydrated, immersed in buffered citrate, and autoclaved. Afterwards, sections were incubated for 30 min in rabbit serum. Incubations with primary antibodies (Table 1) were carried out for 22 h at room temperature. Slides were washed and incubated with biotinylated rabbit anti-mouse immunoglobulin antibodies at a 1:700 dilution and then incubated in PBS/6% hydrogen peroxide for 15 min at room temperature before the addition of an avidin-biotin peroxidase complex (Dakopatts). The

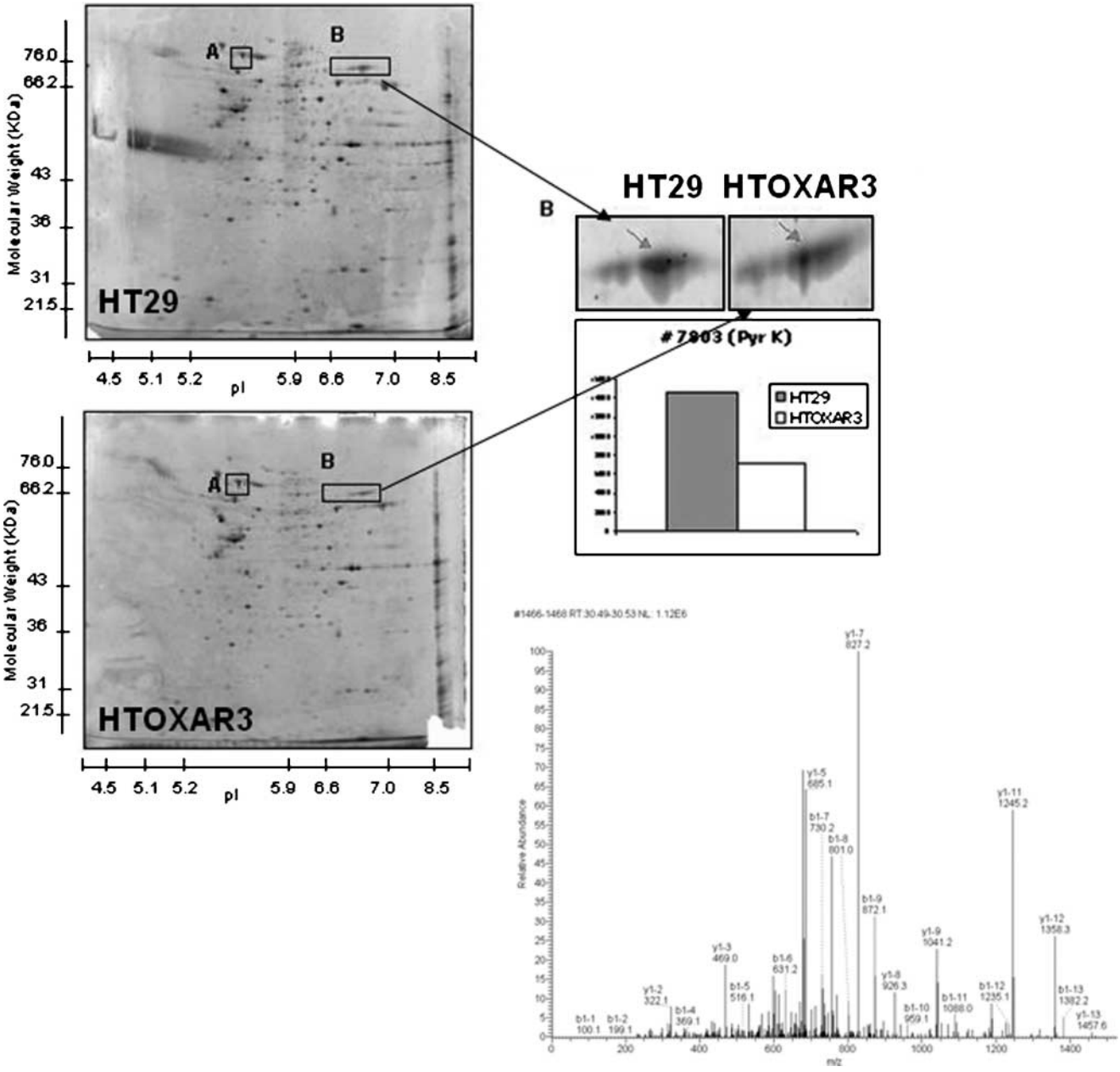

Figure 1 PK-M2 is differentially expressed in oxaliplatin-resistant human colorectal cancer HTOXAR3 cell lines. Two-dimensional gels of protein extracts from HT29 and its oxaliplatin-resistant derivative cell line as well as enlarged partial two-dimensional images showing the different protein patterns in oxaliplatin-resistant cell extracts. Liquid chromatography tandem mass spectrometry analysis of the protein spot differentially expressed in HTOXAR3 oxaliplatin-resistant cells (*bottom*).

chromogen 3,3′-diaminobenzidine tetrachloride (Serva) was applied, and counterstaining was done with Harris hematoxylin. A nonimmnune mouse serum was used as a negative control. Quantification of the results was adapted to the staining patterns of each antibody. For p53 and ki-67, the percentage of positive cells was evaluated as follows: 0, <10%; 1, 10% to 25%; 2, 26% to 50%; or 3, >50%. For bcl-2, tumors were evaluated as positive or negative.

Statistical Analysis

Statistical analysis was carried out using SPSS software v11.5 (SPSS, Inc.). Contingency tables, χ^2, and Fisher's exact tests were used to correlate response and either PK-M2 mRNA expression or clinical variables. The immunohistochemical expression of each marker was assessed in the tissue microarray (three cylinders for each case) and the results were averaged. Differences between groups were considered to be statistically significant at $P < 0.05$. Fisher's exact

test was used to determine the statistical significance of differences between proportions in binary transformed variables (the latter were those variables for which a statistically significant difference or trend was found; they were subsequently recorded). A logistic regression model was established for analysis of the response to chemotherapy as a dummy variable adjusted for PK-M2, p53, bcl-2, and ki-67 as categorical covariates. Covariates of the final model were defined using a block entry methodology. The Spearman test and its associated *r* coefficient were used to assess the correlation between PK-M2 levels and oxaliplatin cytotoxicity in a panel of human colorectal cancer cell lines. The differences were considered statistically significant when two-sided *P* values were less than 0.05.

Results

The isolation of cells resistant to oxaliplatin was previously described (7). Briefly, the isolation was started with an initial continuous exposure of HT29 cells to 2 μmol/L of oxaliplatin. After a period of high mortality, 20% to 30% of cells survived (data not shown). In the following passages, the cell number increased in the presence of oxaliplatin until cells showed doubling times (26–28 hours) equivalent to untreated parental cells (22–24 hours). The growth curve stabilized and no more net mortality occurred after confluence. A similar sequence of events followed with increasing concentrations. The maximum concentration reached was 14 μmol/L of oxaliplatin. The IC_{50} for oxaliplatin was almost 5-fold higher in resistant cells compared with parental cells. Moreover, HTOXAR3 did not exhibit cross-resistance to 5FU, cisplatin, or SN-38 (Table 2). The oxaliplatin-resistant sublines were developed over a 10-month period. These cells were used for the *in vitro* study.

In the pH range 3 to 10, conventional two-dimensional PAGE of HT29 and HTOXAR3 yielded ~1,000 spots for each cell line per fraction (soluble and insoluble). Representative gels and electropherogram are shown in Fig. 1. Using PDQuest software, spots corresponding to proteins overexpressed or down-regulated by 4-fold in the resistant cells compared with sensitive cells were identified. Surprisingly, only a few spots were abundant enough at baseline to be efficiently and unequivocally detected after mass spectrometry and database searches. A SWISS-PROT database search identified one of these proteins as PK-M2 isozyme (molecular weight, 60 kDa; pI 7; SWISS-PROT no. P14786). The coverage percentage of the polypeptidic sequence was >30%, and at least 10 peptides were used for identification in the protein database. The PK-M2 protein was identified in the insoluble fraction as differentially down-regulated in HTOXAR3 cells (Fig. 1). PK-M2 expression was measured in HT29 and HTOXAR3 cells by Western blot analysis. When normalized to actin levels, PK-M2 protein expression was found to be significantly decreased in HTOXAR3,

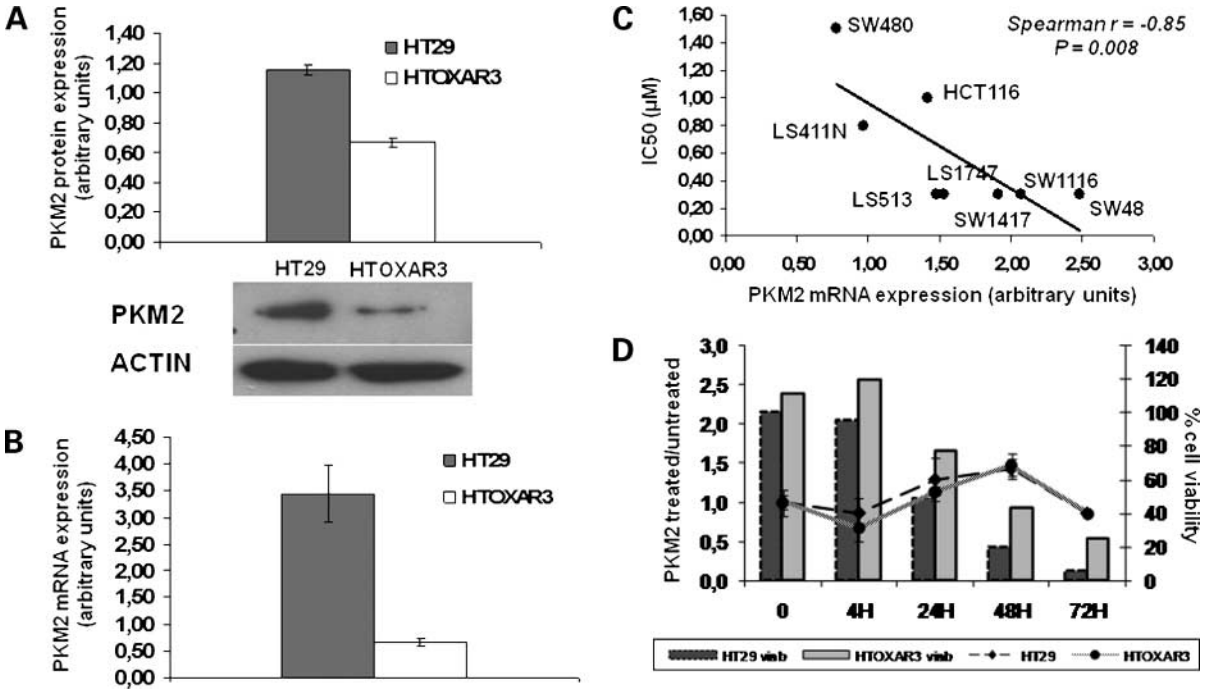

Figure 2 **A,** basal PK-M2 protein levels measured by Western blotting in HT29 and HTOXAR3 cells. Actin was used as an endogenous control. **B,** basal mRNA PK-M2 levels measured by real-time quantitative PCR in HT29 and HTOXAR3 cells. **C,** correlation between PK-M2 mRNA levels and oxaliplatin sensitivity in a panel of eight colorectal cancer cell lines. As HT29 and HTOXAR3 cells exhibited outlying IC_{50} values compared with the rest of the cell lines, we did not include them in the analysis. **D,** PK-M2 mRNA levels (treated/untreated ratio) in response to oxaliplatin-induced damage in HT29 and HTOXAR3 cells. Cells were harvested and treated or untreated with 15 μmol/L of oxaliplatin from 4 to 72 h, the times at which PK-M2 mRNA levels (*points*) and percentage of cell viability (*columns*) were measured.

Table 3 Patients' profiles according to PK-M2 mRNA expression levels

	PK-M2 mRNA expression		
	<0.49	>0.49	*P*
Age, median (range)	59.5 (45–74)	67 (46–81)	
Tumor location			
Colon	6 (60%)	22 (71%)	0.2*
Rectum	4 (40%)	9 (29%)	
Gender			
Male	6 (60%)	17 (55%)	1†
Female	4 (40%)	14 (45%)	
Previous adjuvant CT			
5FU	3 (30%)	9 (29%)	1†
No	7 (70%)	22 (71%)	
Metastatic site			
Liver	7 (70%)	19 (61%)	0.85*
Lung	1 (10%)	3 (10%)	
Other	2 (20%)	9 (29%)	
OR			
Response (CR + PR)	2 (20%)	20 (65%)	0.026†
No response (SD + PD)	8 (80%)	11 (35%)	

Abbreviations: CT, chemotherapy; OR, overall response; CR, complete response; PR, partial response; SD, stable disease; PD, progressive disease.
*χ^2 test *P* value.
†Fisher's exact test *P* value.

thus confirming the results found by proteomic analysis (Fig. 2A).

We further investigated PK-M2 mRNA levels by real-time quantitative PCR. Down-regulation at the transcriptional level was also confirmed in HTOXAR3 cells (Fig. 2B). Indeed, differences between sensitive and resistant cells were higher at the transcriptional level (5-fold) than at the protein level. Moreover, a significant negative correlation between PK-M2 mRNA levels and oxaliplatin sensitivity (Spearman $r = -0.846$, $P = 0.008$) was found in a panel of eight colorectal cancer cell lines (Fig. 2C). To understand the effect of oxaliplatin on *PKM2* gene expression levels, sensitive and resistant cells were treated with 15 μmol/L of oxaliplatin, which corresponds to the IC_{70} and IC_{30} for HT29 and HTOXAR3, respectively, in a 24-hour oxaliplatin exposure experiment. Cells were seeded and left to attach for 24 hours. Then, they were treated with 15 μmol/L of oxaliplatin for 24 hours; the drug-containing medium was removed and changed to a fresh medium. Cells were collected at 0, 4, 24, 48, and 72 hours posttreatment, and PK-M2 mRNA levels, as well as cell viability, were measured. As shown in Fig. 2D, a slight up-regulation of PK-M2 mRNA levels was observed after 4 hours of exposure in both sensitive and resistant cells, indicating a possible role of PK-M2 in oxaliplatin response. After 4 hours of treatment, a decrease in cell viability was also observed. Although PK-M2 basal levels were lower at all times in HTOXAR3 cells (data not shown), the same behavior was observed in both sensitive/resistant pairs. To translate these results into the clinical setting, we studied PK-M2 mRNA expression in 41 colorectal adenocarcinomas from patients who had been treated with oxaliplatin plus 5FU as first-line chemotherapy. PK-M2 protein analysis through immunohistochemistry was difficult to evaluate because its expression was highly abundant in all tumor samples (data not shown). Because we found a correlation between protein and mRNA expression patterns in cell lines, we decided to assess PK-M2 expression at the transcriptional level in tumors. To provide an easily interpretable evaluation of the effect of PK-M2 mRNA expression, gene expression values were divided into quartiles. PK-M2 was detected in all tumors, with values relative to the β-actin internal control ranging 8.36-fold, from 0.25 to 2.09, with a median of 0.67. No differences in clinical features were observed according to PK-M2 mRNA expression levels, but we observed that patients in the bottom quartile (PK-M2 expression < 0.49) had statistically significant lower response rates (Table 3). We chose to validate our results by analyzing three widely used, tumor-associated markers (bcl-2, p53, and ki-67) in a tissue microarray by immunohistochemistry and correlating them with response to chemotherapy as well as with PK-M2 expression. P53 is an important checkpoint of cell cycle regulation that, in part, controls events leading to cell cycle arrest and apoptosis. In contrast, bcl-2 participates in cell cycle regulation, displaying antiapoptotic activity. Ki-67 is an important marker of cell proliferation. As shown in Table 4, 90% of tumors with the lowest PK-M2 mRNA expression (bottom quartile) overexpressed p53 (>25% of cells positive), whereas in the remaining tumors, the percentage showing p53 expression only reached 50% ($P = 0.032$). We did not find any association between bcl-2 or ki-67 protein expression and PK-M2 mRNA levels or clinical features. No association between either of the markers and clinical response was observed (Table 4). In addition, a logistic regression model, including p53, bcl-2, ki-67, and PK-M2 expression as covariates, was established to evaluate the effect of these markers in response to chemotherapy (dependent variable). As shown in Table 5, low PK-M2 expression level was an independent risk factor for no response ($P = 0.015$; odds ratio, 11.09; 95% confidence interval, 1.6–76.73).

Discussion

Oxaliplatin is one of the standard drugs used in colorectal cancer treatment. It is administered in combination with fluoropyrimidines (5FU or capecitabine) in the adjuvant and metastatic setting, and its introduction has achieved response rates over 40% of patients (1). However, typical tumor resistance processes are the main reasons for treatment failure (2). Thus, it is of paramount importance to understand these resistance mechanisms to avoid unnecessary toxicities and increase the response rates. Although several studies have focused on platinum resistance, the majority of them are centered on cisplatin (2) and, in consequence, the mechanisms underlying oxaliplatin resistance remain poorly understood. In the present study, we used a comparative proteomics approach comparing sensitive and oxaliplatin-resistant colorectal cancer cell lines to identify

proteins associated with drug resistance. One such protein was PK-M2, which showed (*a*) a decrease in protein and mRNA levels in HTOXAR3 cells, (*b*) an involvement in oxaliplatin response in sensitive and oxaliplatin-resistant cells, and (*c*) an association with clinical response to oxaliplatin plus 5FU in patients with colorectal cancer. Also, it is worth mentioning that this is one of the few studies in which preclinical results are linked to clinical outcomes.

Pyruvate kinase is a key enzyme in the process of glycolysis, converting phospoenolpyruvate to pyruvate accompanied by ADP to ATP conversion. In mammals, pyruvate kinase exists as four isozymes designated M1, M2, L, and R. These isoforms are differentially expressed in different cell types (10, 11). The M2 type (PK-M2) is predominantly expressed in the fetus, in neoplastic tissues, and in adult stem cells. It can exist as tetrameric or dimeric forms, although the latter is the predominant isoform in tumors. The dimeric form is characterized by a low phosphoenolpyruvate affinity and, indeed, at physiologic phosphoenolpyruvate concentrations, the dimeric form is nearly inactive (11). Besides its role in glycolysis, other functions have been reported for PK-M2. For example, it can influence microtubule stability and interact with phospholipids (12). Recently, it has been reported that, like other glycolytic enzymes (13–16), nuclear translocation of PK-M2 is sufficient and necessary for the induction of apoptosis after treatment with somatostatin analogues or DNA-damaging agents such as H_2O_2 or UV irradiation, and that its kinase activity is not required for this purpose (6). As oxaliplatin is a DNA-damaging agent, similar mechanisms are probably occurring after exposure to this drug. Hoshino and colleagues also showed a role for PK-M2 in cell proliferation regulation via interleukin-3–induced nuclear translocation (17). We report that oxaliplatin-resistant cells had lower basal protein PK-M2 and mRNA levels compared with the parental HT29 cell line. Previous work showed that acquired resistance to cisplatin in gastric carcinoma cell lines is associated with a decrease in PK-M2 levels (18). HTOXAR3 cells were not cross-resistant to cisplatin although the down-regulation in PK-M2 observed in our oxaliplatin-resistant cells may not be sufficient to induce resistance to cisplatin. To our knowledge, this is the first report linking acquired resistance to oxaliplatin with PK-M2 protein and mRNA levels in colorectal cancer. The decreased PK-M2 levels found in resistant cells could be important to avoiding programmed cell death after oxaliplatin exposure. It is well known that adequate ATP levels are necessary for the initiation and progression of apoptosis (19, 20). Therefore, the decreased levels of proteins involved in glycolytic generation of ATP may play a role in the protection of HTOXAR3 from the activation of apoptotic pathways in response to oxaliplatin treatment. It is worth mentioning that α-enolase, another glycolytic enzyme, was also found to be down-regulated in HTOXR3 cells (data not shown). On the other hand, nuclear translocation of PK-M2 is sufficient to induce cell death that is caspase independent, isoform specific, and independent of its enzymatic activity (6). Therefore, down-regulation of PK-M2 in HTOXAR3 indicates that this is a mechanism that may impart protection from oxaliplatin-induced cell death. Similarly, HEK293 cells stably overexpressing PK-M2 showed an increased sensitivity to TT-232 (a somatostatin analogue) when compared with HEK293 cells (6). We also report a negative correlation between PK-M2 mRNA levels and oxaliplatin IC_{50} in a panel of eight colorectal cancer cell lines. We observed an increase in PK-M2 mRNA levels after exposure to 15 μmol/L of oxaliplatin in both sensitive and resistant cells, possibly indicating a positive transcriptional regulation of PK-M2 as a consequence of oxaliplatin-induced DNA damage. However, the maintenance of PK-M2 up-regulation in the resistant cell line in the presence of oxaliplatin somehow corroborates that a decrease in PK-M2 levels is enough to affect its apoptotic capacity. Our results are in line with previous studies in the literature demonstrating that the silenced expression of the *PKM2* gene has a direct involvement in cisplatin resistance (18). Further studies including PK-M2 overexpression and/or silencing in these cell lines and their correlation with response to oxaliplatin could further clarify this point. Our study, for the first time, shows the prognostic value of PK-M2 expression as a marker of response to oxaliplatin-based therapy. It is important to note that 80% of the patients whose primary tumors had lower PK-M2 mRNA basal levels did not respond to first-line chemotherapy treatment with oxaliplatin/5FU regimen. Taking into account that our oxaliplatin-resistant cells did not exhibit cross-resistance to 5FU, PK-M2 could be considered as a predictive

Table 4 Association of p53, ki-67, and bcl-2 protein expression with PK-M2 mRNA levels and response to therapy

	Bcl-2			p53			Ki-67		
	Present	Absent	*P*	<50%	>50%	*P*	<50%	>50%	*P*
PK-M2									
<0.49	4 (40%)	6 (60%)	1*	1 (10%)	9 (90%)	0.032*	1 (10%)	9 (90%)	1*
>0.49	13 (42%)	18 (58%)		15 (50%)	15 (50%)		4 (13%)	27 (87%)	
OR									
R	8 (47%)	14 (58%)	0.54*	10 (62.5%)	12 (50%)	0.54†	4 (80%)	18 (50%)	0.35†
NR	9 (53%)	10 (42%)		6 (37.5%)	12 (50%)		1 (20%)	18 (50%)	

Abbreviations: OR, overall response; R, response; NR, no response.
*Fisher's exact test–associated *P* value.
†χ^2 test–associated *P* value.

Table 5 Logistic regression model for response to chemotherapy

Marker	OR (95% CI)	*P*
PK-M2 >0.49	11.09 (1.6–76.72)	0.015
P53 <50%	1.65 (0.34–7.99)	0.53
Ki-67 <50%	0.2 (0.013–3.23)	0.26
Bcl-2 negative	0.52 (0.12–2.22)	0.38

Abbreviations: OR, odds ratio; 95% CI, 95% confidence interval.

factor for oxaliplatin-based treatment. In these patients, high p53 levels were associated with low levels of PK-M2. Although these two factors would have a negative additive effect on response, high p53 levels did not predict for a worse response in our patient cohort. Indeed, in a logistic regression model, only PK-M2 levels were identified to be an independent risk factor. Therefore, our results agree with those showing that p53 is not a useful marker for monitoring chemotherapy response in colorectal cancer (21). On the other hand, no association was found with bcl-2, which is in accordance with Steták et al., who reported a PK-M2–induced bcl-2–independent cell death (6).

Although caution is needed when interpreting these results due to the small number of patients evaluated, our data suggest that the molecular profile of the primary tumor could be used as a marker for clinical outcome in patients with colon adenocarcinomas treated with oxaliplatin plus 5FU. It is important to note that drug resistance is a multifactorial process and that other proteins were also found to be altered in HTOXAR3 cells. Even so, to our knowledge, this is the first translational study correlating PK-M2 expression and response to oxaliplatin-based chemotherapy. In the light of recent results demonstrating that the M2 isoform of pyruvate kinase protein is critical for rapid tumor growth (22), and necessary for aerobic glycolysis and tumorigenesis (23), further studies are warranted to elucidate the molecular mechanisms underlying PK-M2 expression in oxaliplatin response and resistance.

Disclosure of Potential Conflicts of Interest

No potential conflicts of interest were disclosed.

References

1. Kelland L. The resurgence of platinum-based cancer chemotherapy. Nat Rev Cancer 2007;7:573–84.

2. Rabik CA, Dolan ME. Molecular mechanisms of resistance and toxicity associated with platinating agents. Cancer Treat Rev 2007;33:9–23.

3. Martinez-Balibrea E, Abad A, Aranda E, et al. Pharmacogenetic approach for capecitabine or 5-fluorouracil selection to be combined with oxaliplatin as first-line chemotherapy in advanced colorectal cancer. Eur J Cancer 2008;44:1229–37.

4. Martinez-Cardús A, Martinez-Balibrea E, Bandrés E, et al. Pharmacogenomic approach for the identification of novel determinants of resistance to oxaliplatin in colon cancer. Mol Cancer 2009;8:194–202.

5. Plebani M. Proteomics: the next revolution in laboratory medicine? Clin Chim Acta 2005;357:113–22.

6. Steták A, Veress R, Ovadi J, Csermely P, Keri G, Ullrich A. Nuclear translocation of the tumor marker pyruvate kinase M2 induces programmed cell death. Cancer Res 2007;67:1602–8.

7. Plasencia C, Martinez-Balibrea E, Martinez-Cardus A, Quinn DI, Abad A, Neamati N. Expression analysis of genes involved in oxaliplatin response and development of oxaliplatin-resistant HT29 colon cancer cells. Int J Oncol 2006;29:225–35.

8. Alley MC, Scudiero DA, Monks A, et al. Feasibility of drug screening with panels of human tumor cell lines using a microculture tetrazolium assay. Cancer Res 1988;48:589–601.

9. Taron M, Rosell R, Felip E, et al. BRCA1 mRNA expression levels as an indicator of chemoresistance in lung cancer. Hum Mol Genet 2004;13:2443–9.

10. Tanaka T, Harano Y, Sue F, Morimura H. Crystallization, characterization and metabolic regulation of two types of pyruvate kinase isolated from rat tissues. J Biochem (Tokyo) 1967;62:71–91.

11. Mazurek S, Boschek CB, Hugo F, Eigenbrodt E. Pyruvate kinase type M2 and its role in tumor growth and spreading. Semin Cancer Biol 2005;15:300–8.

12. Vertessy BG, Bankfalvi D, Kovacs J, Low P, Lehotzky A, Ovadi J. Pyruvate kinase as a microtubule destabilizing factor *in vitro*. Biochem Biophys Res Commun 1999;254:430–5.

13. Dastoor Z, Dreyer JL. Potential role of nuclear translocation of glyceraldehyde-3-phosphate dehydrogenase in apoptosis and oxidative stress. J Cell Sci 2001;114:1643–53.

14. Sawa A, Khan AA, Hester LD, Snyder SH. Glyceraldehyde-3-phosphate dehydrogenase: nuclear translocation participates in neuronal and nonneuronal cell death. Proc Natl Acad Sci U S A 1997;94:11669–74.

15. Ronai Z. Glycolytic enzymes as DNA binding proteins. Int J Biochem 1993;25:1073–6.

16. Tarze A, Deniaud A, Le Bras M, et al. GAPDH, a novel regulator of the pro-apoptotic mitochondrial membrane permeabilization. Oncogene 2007;26:2606–20.

17. Hoshino A, Hirst JA, Fujii H. Regulation of cell proliferation by interleukin-3-induced nuclear translocation of pyruvate kinase. J Biol Chem 2007;282:17706–11.

18. Yoo BC, Ku JL, Hong SH, et al. Decreased pyruvate kinase M2 activity linked to cisplatin resistance in human gastric carcinoma cell lines. Int J Cancer 2004;108:532–9.

19. Nicotera P, Leist M. Energy supply and the shape of death in neurons and lymphoid cells. Cell Death Differ 1997;4:435–42.

20. Nicotera P, Leist M. Mitochondrial signals and energy requirement in cell death. Cell Death Differ 1997;4:516.

21. Duffy MJ, van Dalen A, Haglund C, et al. Tumour markers in colorectal cancer: European Group on Tumour Markers (EGTM) guidelines for clinical use. Eur J Cancer 2007;43:1348–60.

22. Christofk HR, Vander Heiden MG, Wu N, Asara JM, Cantley LC. Pyruvate kinase M2 is a phosphotyrosine-binding protein. Nature 2008;452:181–6.

23. Christofk HR, Vander Heiden MG, Harris MH, et al. The M2 splice isoform of pyruvate kinase is important for cancer metabolism and tumour growth. Nature 2008;452:230–3.